dation of (OEP)Ir(C_3H_7)(CO) indicate that (OEP)Ir(CO)ClO_4 is the singly oxidized product. A similar spectral result is obtained during oxidation of (OEP)Ir(C_8H_{13})(CO) and leads to the formation of (OEP)Ir(CO)ClO_4.[19]

The cyclic voltammograms for oxidation of (OEP)Ir(C_3H_7)(PPh_3) and (OEP)Ir(C_3H_7)(P(OEt)$_3$) are irreversible, and this is consistent with the irreversible spectral changes obtained upon oxidation of the complexes in a thin-layer cell. The resulting spectral changes during oxidation of (OEP)Ir(C_3H_7)(PPh_3) are illustrated in Figure 9. The original six-coordinate porphyrin exhibits a split Soret band at 367 and 423 nm and two Q bands at 530 and 547 nm. A new Soret band appears at 397 nm, and two well-defined Q bands appear at 512 and 545 nm after oxidation at 0.70 V. Six isosbestic points are obtained during oxidation, but these changes were not reversible and no spectral changes were monitored during the reverse controlled-potential reduction at 0.0 V.

Infrared spectroelectrochemistry was used in order to ascertain the final site of the electron transfer in (OEP)Ir(C_3H_7) and (OEP)Ir(C_3H_7)(L), where L = py, *N*-MeIm, or Me_2SO. Cation radicals of octaethylporphyrins[43] have been characterized as having a diagnostic absorption band between 1570 and 1520 cm^{-1}, but infrared spectra recorded after the one-electron oxidation of (OEP)Ir(C_3H_7) and (OEP)Ir(C_3H_7)(Me_2SO) do not show any absorptions between 1620 and 1480 cm^{-1}. This agrees with the UV-visible results and suggests that the site of the electron abstraction may not be at the porphyrin π ring system.

Finally, the products of controlled-potential oxidation were also monitored by ESR spectroscopy. Complete electrolysis required 1.0 ± 0.1 electrons for oxidation of each (OEP)Ir(C_3H_7)(L) complex. When a sixth ligand was not bound to (OEP)Ir(C_3H_7) or when L was py, *N*-MeIm, or Me_2SO, the oxidized product, $[(OEP)Ir(C_3H_7)]^+$ or $[(OEP)Ir(C_3H_7)(L)]^+$, exhibited an ESR signal centered at $g = 2.00$ with a peak-to-peak separation between 15 and 40 G.

Acknowledgment. The support of the National Science Foundation (Grant CHE-8515411) is gratefully acknowledged. We also acknowledge discussions with Dr. P. F. Blanchet.

Registry No. **1**, 120086-16-0; **2**, 120120-20-9; (OEP)Ir(C_3H_7), 120086-15-9; (OEP)Ir(C_3H_7)(py), 120086-17-1; (OEP)Ir(C_3H_7)(*N*-MeIm), 120086-18-2; (OEP)Ir(C_3H_7)(CO), 120086-19-3; (OEP)Ir(C_3H_7)(P(OEt)$_3$), 120086-20-6; (OEP)Ir(C_3H_7)(NEt_3), 120086-21-7; (OEP)Ir(CO)Cl, 68324-58-3; $CH_3(CH_2)_2I$, 107-08-4.

Supplementary Material Available: Tables of hydrogen atomic coordinates, anisotropic thermal parameters, and all intramolecular distances and angles (15 pages); listings of observed and calculated structure factors (60 pages). Ordering information is given on any current masthead page.

---

(43) Shimonmura, E. T.; Phillippi, M. A.; Goff, H. M. *J. Am. Chem. Soc.* **1981**, *103*, 6778.

Contribution from the Department of Chemistry, University of Houston, Houston, Texas 77204-5641,
Laboratoire de Chimie Physique Générale, Faculté des Sciences de Rabat, Université Mohammed V, Rabat, Morocco,
and Laboratoire de Synthèse et d'Electrosynthèse Organométallique, Associé au CNRS (UA 33),
Faculté des Sciences "Gabriel", Université de Dijon, 21100 Dijon, France

Electrochemistry of Nickel "Picket Fence" Porphyrin. Electrogeneration and Spectral Characterization of Nickel Complexes in Unusual Oxidation States

K. M. Kadish,*[,1a] D. Sazou,[1a] G. B. Maiya,[1a] B. C. Han,[1a] Y. M. Liu,[1a] A. Saoiabi,[1b] M. Ferhat,[1b] and R. Guilard*[,1c]

Received November 30, 1988

The electrochemical and spectroelectrochemical characterization of nickel(II) *meso*-$\alpha,\alpha,\alpha,\alpha$-tetrakis(*o*-pivalamidophenyl)porphyrin, (TpivPP)Ni, in dichloromethane, benzonitrile, and tetrahydrofuran is reported. The oxidative behavior of this complex is different from that of all previously studied nickel porphyrins. The complex is reversibly oxidized by three electrons in two steps and generates as a final product $[(TpivPP)Ni]^{3+}$, which was characterized as a Ni(IV) cation radical in solution by both UV-visible and ESR spectroscopy. The electroreduction of (TpivPP)Ni involves a stepwise addition of two electrons to the porphyrin π ring system. The electrogenerated $[(TpivPP)Ni]^-$ was characterized by UV-visible and ESR spectroscopy in THF and was shown to catalyze the electrochemical reduction of methyl iodide.

Introduction

The electrochemistry of "picket fence", "basket handle", and binary "face to face" porphyrins has been reported.[2-8] These compounds are structurally similar in that they all have amide- or ether-linked chains attached to the ortho position of the four phenyl groups of a tetraphenylporphyrin macrocycle. Most electrochemical studies of these compounds involved characterization of iron[2,4-6] and cobalt[7] derivatives, and studies on the electron-transfer reactivity of related porphyrins with other central metals are sparse.[3,8] It has been shown that the "picket fence" porphyrin (TpivPP)Cu, where TpivPP is the dianion of *meso*-$\alpha,\alpha,\alpha,\alpha$-tetrakis(*o*-pivalamidophenyl)porphyrin, as well as amide-linked "basket handle" porphyrins of Cu, Zn, and Mg undergo a reversible overall two-electron oxidation in nonaqueous media.[3] No other "picket fence" porphyrins have been investigated with respect to their oxidative behavior, nor has the reductive behavior of any metalated "superstructured" porphyrin containing other than iron or cobalt been reported.[9]

This present study reports the synthesis and electrochemistry of (TpivPP)Ni in CH_2Cl_2, PhCN, and THF. This complex, whose structure is shown in Figure 1, is of special interest in under-

---

(1) (a) University of Houston. (b) Université Mohammed V. (c) Université de Dijon.

(2) Lexa, D.; Momenteau, M.; Rentien, P.; Rytz, G.; Savéant, J.-M.; Xu, F. *J. Am. Chem. Soc.* **1984**, *106*, 4755.

(3) Lexa, D.; Maillard, P.; Momenteau, M.; Savéant, J.-M. *J. Am. Chem. Soc.* **1984**, *106*, 6321.

(4) Lexa, D.; Momenteau, M.; Savéant, J.-M.; Xu, F. *Inorg. Chem.* **1985**, *24*, 122.

(5) Lexa, D.; Momenteau, M.; Savéant, J.-M.; Xu, F. *J. Am. Chem. Soc.* **1986**, *108*, 6937.

(6) Gueutin, C.; Lexa, D.; Momenteau, M.; Savéant, J.-M.; Xu, F. *Inorg. Chem.* **1986**, *25*, 4294.

(7) Collman, J. P.; Marrocco, M.; Elliott, C. M.; L'Her, M. *J. Electroanal. Chem. Interfacial Electrochem.* **1981**, *124*, 113.

(8) Becker, J. Y.; Dolphin, D.; Paine, J. B.; Wijesekera, T. *J. Electroanal. Chem. Interfacial Electrochem.* **1984**, *164*, 335.

(9) The electrochemical reduction of the free base porphyrin, (TpivPP)H_2, was investigated in DMF by: Bump, C. M. Ph.D. Dissertation, The Pennsylvania State University, 1979. (TpivPP)H_2 is reduced via two successive one-electron transfers, and the overall reduction follows an ECEC mechanism. The first chemical step was assigned to a conformational change of the complex and the second step to a protonation reaction that resulted from trace H_2O in the DMF and led to the formation of a phlorin, the final electroreduction product.

0020-1669/89/1328-2542$01.50/0 © 1989 American Chemical Society

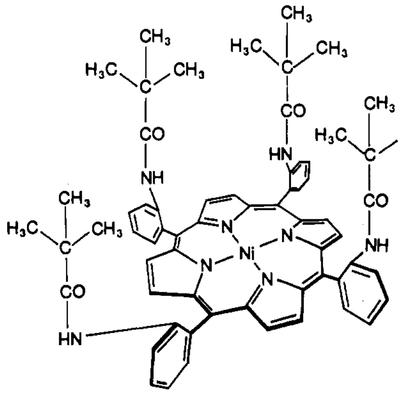

Figure 1. Structure of (TpivPP)Ni.

standing how changes in the macrocycle can lead to changes in the site of oxidation or reduction in nickel porphyrins[10-15] and the related chlorins and isobacteriochlorins.[15-19] Either a d^9 Ni(I) porphyrin or a Ni(II) porphyrin anion radical may be generated upon reduction of the original Ni(II) species. The specific site of electroreduction will depend upon the nature of the conjugated π ring system and possibly the solvent and supporting electrolyte system.[10-18,20]

The relative energy levels of the central metal and the porphyrin macrocycle, as well as the specific process or processes leading to chemical or electrochemical generation of a Ni(III) macrocycle, have also been a point of continued interest and debate in the literature.[10-15,19,20] As will be shown in this study, three electrons can be reversibly abstracted in two steps from (TpivPP)Ni, and this leads to formation of a Ni(IV) porphyrin cation radical in solution. The presence of a Ni(IV) center in $(OEP)Ni(Br)_2$ (where OEP is the dianion of octaethylporphyrin) was tentatively suggested in the literature. However, the authors noted that this species was not well characterized,[21] and the properties of a genuine Ni(IV) cation radical have yet to be described. The spectral properties of electrogenerated $[(TpivPP)Ni]^{2+}$, $[(TpivPP)Ni]^{3+}$, and $[(TpivPP)Ni]^-$ as well as the reactivity of $[(TpivPP)Ni]^-$ with methyl iodide are also reported in this work.

Experimental Section

Instrumentation and Methods. Cyclic voltammograms were obtained with an IBM Model EC 225 voltammetric analyzer and an Omnigraphic 2000 X-Y recorder using a three-electrode system. The working electrode was a platinum button of area 0.80 mm^2. A platinum wire served as the counter electrode, and a homemade aqueous saturated calomel electrode (SCE) was used as the reference electrode, which was separated from the bulk solution by a glassy diaphragm connected to a bridge filled with the electrolyte solution. All potentials are referenced vs SCE. Controlled-potential electrolysis was carried out with an EG&G Princeton Applied Research Model 174A potentiostat/Model 179 coulometer system, which was coupled with an EG&G Princeton Applied Research Model RE-0074 time-base X-Y recorder.

Spectroelectrochemical measurements were made with a Tracor-Northern 1710 optical spectrometer/multichannel analyzer, which was coupled with a TN-1710-24 floppy disk system for spectral acquisitions. The utilized optically transparent thin-layer electrode is described in the literature.[22] UV-visible spectra of the complexes before electrooxidation or electroreduction were also recorded with an IBM-9430 spectrophotometer.

ESR spectra were taken with an IBM Model ER 100D spectrometer equipped with an ER 040-X microwave bridge and an ER 080 power supply. For low-temperature measurements, the cavity was cooled by a stream of liquid nitrogen that was constantly passed through a variable-temperature insert. The g values were measured relative to diphenylpicrylhydrazyl (DPPH; $g = 2.0037 \pm 0.0002$). ^1H NMR spectra were taken with a QE 300 spectrometer, and chemical shifts are reported with respect to tetramethylsilane.

Reagents. Dichloromethane (CH_2Cl_2) obtained from Aldrich Chemical Co. was twice distilled over CaH_2 or P_2O_5. Tetrahydrofuran (THF), obtained from Fisher Scientific Chemical Co., was distilled at first over CaH_2 and then over sodium/benzophenone prior to use. Benzonitrile (PhCN) was purchased from Aldrich Chemical Co. and vacuum-distilled over P_2O_5 just prior to use. Tetra-*n*-butylammonium perchlorate (TBAP) and tetra-*n*-butylammonium hexafluorophosphate ($(TBA)PF_6$), purchased from Fluka Chemical Co., were recrystallized from absolute ethyl alcohol and dried in a vacuum oven at 40 °C prior to use. Methyl iodide was purchased from Aldrich Chemical Co. and was used directly as received. Further purification of CH_3I does not affect its reactivity with $[(P)Ni]^-$ complexes.[17] In addition, 1 mM solutions of CH_3I showed no electrochemical reactivity or trace of electrochemically active impurities over the range of investigated potentials.

All electrochemical and spectral measurements were carried out at 22 ± 1 °C, unless otherwise specified. The synthesis of (TpivPP)Ni is described below.

(TpivPP)Ni. Free-base *meso*-$\alpha,\alpha,\alpha,\alpha$-tetrakis(*o*-pivalamidophenyl)-porphyrin ($(TpivPP)H_2$) was prepared according to the method of Collman et al.[23] A 150-mg amount of $(TpivPP)H_2$, 264 mg of $NiCl_2{\cdot}6H_2O$, and 100 mL of DMF were refluxed for 1 h. After complete metalation, the solvent was evaporated and the product dissolved in CH_2Cl_2. The CH_2Cl_2 extract was washed with water in order to remove unreacted $NiCl_2{\cdot}6H_2O$ and trace DMF. (TpivPP)Ni was obtained in a yield of 70%. Thin-layer chromatography experiments with silica gel and either 95% CH_2Cl_2/5% MeOH or neat DMF showed only a single spot for the complex. UV-visible spectral data for (TpivPP)Ni in CH_2Cl_2 (λ_{max}, nm (ϵ)): 411 (89.7×10^3), 524 (7.2×10^3), 556 (2.7×10^3), 614 (0.9×10^3). ^1H NMR data for (TpivPP)Ni (ppm): 8.74 (m, 12 H, β-pyrrole and -NHCO), 7.27 (m, 16 H, phenyl), 0.16 (m, 36 H, pivaloyl).

Results and Discussion

Electrooxidation of (TpivPP)Ni and Electrogeneration of $[(TpivPP)Ni^{IV}]^{3+}$. The electrooxidation of (TpivPP)Ni differs from that of all previously investigated nickel porphyrins[10-15,19,20] in that the compound is reversibly oxidized by three electrons in two steps. The first oxidation of (TpivPP)Ni involves an overall two-electron transfer and gives $[(TpivPP)Ni]^{2+}$ as a final product. The second oxidation proceeds via a one-electron-transfer process and leads to $[(TpivPP)Ni]^{3+}$ as a final oxidation product as shown in Scheme I.

Scheme I

$$(TpivPP)Ni \underset{}{\overset{-2e^-}{\rightleftharpoons}} [(TpivPP)Ni]^{2+} \overset{-e^-}{\rightleftharpoons} [(TpivPP)Ni]^{3+}$$

Evidence for the above sequence of reactions comes from an analysis of cyclic voltammograms in CH_2Cl_2 and normal pulse voltammograms in PhCN. The cyclic voltammograms of (TpivPP)Ni are shown in Figure 2a and illustrate the two oxidations that occur at $E_{1/2} = 1.19$ and 1.41 V in CH_2Cl_2 containing 0.1 M $(TBA)PF_6$. The first oxidation (process I) is quasireversible to irreversible at scan rates higher than 0.05 V/s and involves an overall two-electron abstraction as ascertained by analysis of the peak current maximum and thin-layer coulometry, which gave 2.0 ± 0.1 electrons abstracted. The second oxidation (process II) is reversible at all scan rates up to 100 V/s.

The first oxidation of (TpivPP)Ni has a peak current maximum by cyclic voltammetry which is double that of the first reduction under the same experimental conditions and is approximately double that of the second oxidation (see Figure 2a). Process I is reversible by cyclic voltammetry at scan rates <0.05 V/s, and this is illustrated in Figure 2 by the cyclic voltammogram at 0.02

---

(10) Kadish, K. M. *Prog. Inorg. Chem.* **1986**, *34*, 435.
(11) Wolberg, A.; Manassen, J. *Inorg. Chem.* **1970**, *9*, 2365.
(12) Dolphin, D.; Niem, T.; Felton, R. H.; Fujita, I. *J. Am. Chem. Soc.* **1975**, *97*, 5288.
(13) Johnson, E. C.; Niem, T.; Dolphin, D. *Can. J. Chem.* **1978**, *56*, 1381..
(14) Kadish, K. M.; Morrison, M. M. *Inorg. Chem.* **1976**, *15*, 980.
(15) Chang, D.; Malinski, T.; Ulman, A.; Kadish, K. M. *Inorg. Chem.* **1984**, *23*, 817.
(16) Stolzenberg, A. M.; Stershic, M. T. *Inorg. Chem.* **1987**, *26*, 3082.
(17) Stolzenberg, A. M.; Stershic, M. T. *J. Am. Chem. Soc.* **1988**, *110*, 5397.
(18) Stolzenberg, A. M.; Stershic, M. T. *J. Am. Chem. Soc.* **1988**, *110*, 6391.
(19) Stolzenberg, A. M.; Stershic, M. T. *Inorg. Chem.* **1988**, *27*, 1614.
(20) Kadish, K. M.; Sazou, D.; Liu, Y. M.; Saoiabi, A.; Ferhat, M.; Guilard, R. *Inorg. Chem.* **1988**, *27*, 1198.
(21) Antipas, A.; Gouterman, M. *J. Am. Chem. Soc.* **1983**, *105*, 4896.
(22) Lin, X. Q.; Kadish, K. M. *Anal. Chem.* **1985**, *57*, 1498.
(23) Collman, J. P.; Gagne, R.R.; Reed, C. A.; Halbert, T. R.; Lang, G.; Robinson, W. T. *J. Am. Chem. Soc.* **1975**, *97*, 1427.

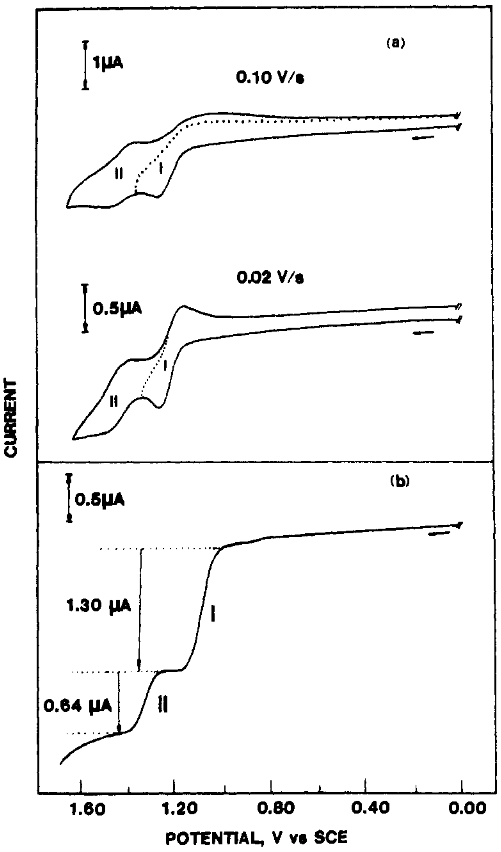

Figure 2. Current-potential curves for the oxidation of 10^{-3} M (TpivPP)Ni by (a) cyclic voltammetry in CH_2Cl_2, 0.1 M $(TBA)PF_6$ at scan rates of 0.10 and 0.02 V/s and (b) normal pulse voltammetry in PhCN, 0.1 M TBAP at a scan rate of 0.005 V/s and a pulse time of 0.1 s.

V/s. The peak potential for this oxidation shifts positively by 60 mV for each 10-fold increase in sweep rate above 0.10 V/s, but $E_{\rm p}$ for process II remains invariant with increase in sweep rate between 0.10 and 0.50 V/s. The peak separation $|E_{\rm p} - E_{{\rm p}/2}| = 95 \pm 5$ mV for process I at low scan rates is consistent with a quasireversible one-electron transfer as the rate-controlling step in the overall two-electron oxidation of (TpivPP)Ni..

Similar oxidations occur in CH_2Cl_2 solutions containing TBAP as supporting electrolyte, but under these conditions the room-temperature oxidation potentials are shifted to $E_{\rm p} = 1.16$ V and $E_{1/2} = 1.27$ V. This effect of supporting electrolyte has been observed for the oxidation of other $(P)Ni^{II}$ complexes.[15]

A similar sequence of steps also occurs for oxidation of the complex in PhCN containing 0.1 M TBAP. The initial two-electron oxidation occurs at $E_{1/2} = 1.08$ V in this solvent, while the following one-electron-transfer process is located at $E_{1/2} = 1.32$ V. This is illustrated by the normal pulse voltammogram shown in Figure 2b. Analysis of the current-potential curve for the first oxidation obtained by rotating-disk voltammetry gives a straight-line slope of 0.112 V for a plot of E vs log $[i/(i_{\rm d} - i)]$. The theoretical values for reversible one- and two-electron transfers are 0.060 and 0.030 V, respectively, and the experimentally obtained 0.112 V thus indicates a slow (rate-determining)charge-transfer step in process I. This result is consistent with the cyclic voltammetric data, which give an $|E_{\rm pa} - E_{\rm pc}|$ value of 95 ± 5 mV at a scan rate of 0.02 V/s. The limiting current for the first oxidation by normal pulse voltammetry (1.30 μA) is double that for the second oxidation (0.64 μA) and is thus consistent with the overall sequence of steps shown in Scheme I.

A direct abstraction of two electrons has also been observed for Mg(II), Cu(II), and Zn(II) complexes of amide-linked basket-handle porphyrins.[3] However, in these cases, the two-electron-oxidation process was reversible and this was explained in terms of an electrochemical ECEC type mechanism. The nature of the chemical steps was not ascertained, but rate-determining structural changes involving the amide groups were suggested. A similar mechanism involving the pivalamidophenyl groups may explain the quasireversible two-electron transfer observed for (TpivPP)Ni. However, at the present time, no direct evidence exists for ascertaining this hypothesis.

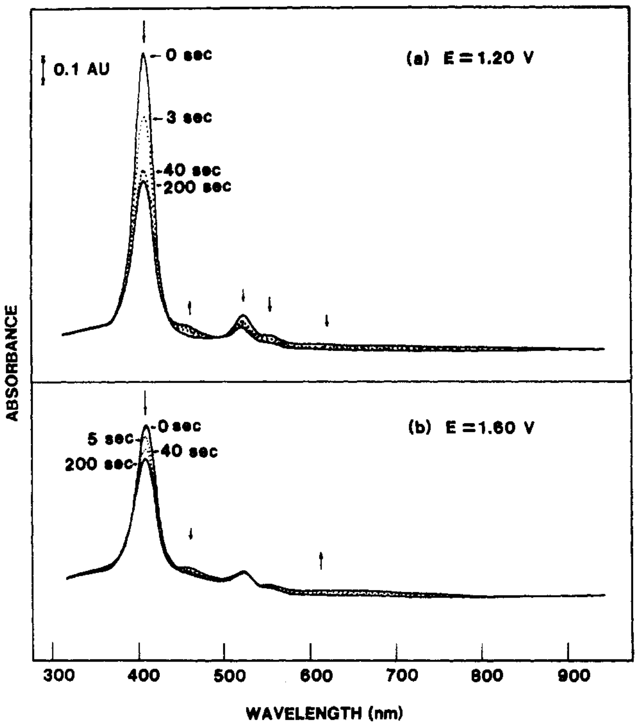

Figure 3. Time-resolved thin-layer spectral changes during controlled-potential oxidation of (TpivPP)Ni in CH_2Cl_2, 0.2 M TBAP.

Several different electrochemical mechanisms involving a conversion of Ni(II) to Ni(III) porphyrins,[10-15] chlorins,[15,19] and isobacteriochlorins[19] have been discussed in the literature. A Ni(III) derivative may be generated as a product of the first oxidation at low temperature[11-13] or as a product of the second oxidation at room temperature.[10,14,15] In the first case, the reaction proceeds via an intramolecular electron transfer involving a Ni(II) porphyrin cation radical,[11-13] while in the second case an intramolecular transfer may or may not be involved in the generation of a Ni(III) porphyrin cation radical.

The key point in all previous studies is that the energy levels of the relevant porphyrin orbitals and those of the central Ni(II) ion were similar and could be changed with respect to each other by only subtle changes in the porphyrin π ring system or by changes in the solution temperature. These variations led to changes in the exact sequence of electron-transfer steps, but in almost all cases, a Ni(III) cation radical was generated after the global abstraction of two electrons from the initial Ni(II) porphyrin complex.

In this present study, the first oxidation of the Ni(II) porphyrin (process I) involves an overall two-electron abstraction, which can lead to either $[(TpivPP)Ni^{III}]^{2+}$ or $[(TpivPP)Ni^{II}]^{2+}$ as a final electrooxidation product. The UV-visible spectra of numerous porphyrin cation radicals and dications have been reported,[15,24] and thus spectroelectrochemical monitoring of the oxidation should enable a determination of the exact product in this overall two-electron oxidation.

Figure 3a illustrates time-resolved UV-vis spectra taken during controlled-potential oxidation of (TpivPP)Ni at 1.20 V. The spectral changes are reversible, and the final spectrum suggests that $[(TpivPP)Ni^{III}]^{2+}$ is the ultimate oxidation product in process I. This assignment is made on the basis of the small observed decrease of the Soret band at 411 nm. This type of behavior is not characteristic of porphyrin dication formation which would

---

(24) Felton, R. H. In *The Porphyrins*; Dolphin, D., Ed.; Academic Press: New York, 1978; Vol. 5, p 81.

Table I. UV-Visible Data for (TpivPP)Ni and Its Reduction or Oxidation Products in CH_2Cl_2 or THF Containing 0.2 M TBAP

electrode process[a]	solvent	λ, nm ($10^{-3}\epsilon$, M^{-1} cm^{-1})				
none	CH_2Cl_2	411 (89.7)	524 (7.2)	556 (2.7)	614 (0.9)	
reacn I	CH_2Cl_2	411 (50.4)	458 (7.0)	524 (6.5)	556 (1.8)	
reacn II	CH_2Cl_2	411 (40.0)	458 (6.1)	524 (6.5)	556 (2.3)	653 (0.4)
none	THF	412 (106.8)	527 (9.8)	557 (3.6)	617 (1.3)	
reacn III	THF	421 (56.5)	527 (5.1)	557 (2.8)	617 (3.1)	860 (1.5)
reacn IV	THF	425 (23.0)	447 (30.6)			793 (4.2)

[a] See cyclic voltammograms in Figures 2 and 5, which identify the specific redox processes.

Scheme II

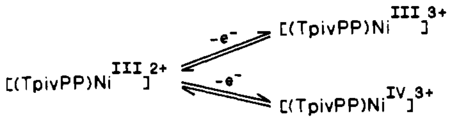

Scheme III

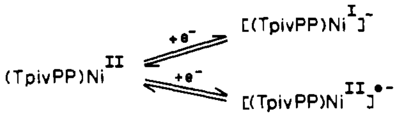

be accompanied by a large decrease in the Soret band's molar absorptivity.[15] There is no ESR signal after the two-electron bulk electrooxidation of (TpivPP)Ni at +1.13 V, but a coupling of the unpaired electron on the Ni(III) center and that on the porphyrin macrocycle of $[(TpivPP)Ni^{III}]^{2+}$ would account for this lack of an ESR signal.[24,25]

The second oxidation of $[(TpivPP)Ni^{III}]^{2+}$ occurs at $E_{1/2} = 1.27$ V in CH_2Cl_2, 0.1 M TBAP and can lead to either a Ni(III) porphyrin dication or a Ni(IV) cation radical as shown in Scheme II.

The formation of a Ni(III) porphyrin dication should be accompanied by a characteristic decrease in the Soret and UV-visible bands of the electronic absorption spectra.[15] The electrooxidized complex should also have an ESR spectrum characteristic of Ni(III); i.e., $g_\perp > g_\parallel$, where $g_\perp$ is between 2.200 and 2.170 and $g_\parallel$ is close to 2.020.[26] In contrast, $[(TpivPP)Ni^{IV}]^{3+}$ should have a porphyrin π-cation-radical ESR spectrum and a UV-visible spectrum similar to spectra of other porphyrin cation radicals, which for the case of $[(TPP)Ni^{II}]^{+}$ has bands at 410, 606, 641, and 750 nm.[15]

The actual time-resolved UV-visible spectrum obtained during controlled potential oxidation of $[(TpivPP)Ni]^{2+}$ is shown in Figure 3b. The final UV-visible spectrum of $[(TpivPP)Ni]^{3+}$ at $E_{app} = 1.60$ V is obtained after 200 s of electrolysis and is somewhat similar to the initial spectrum of $[(TpivPP)Ni]^{2+}$ in the Soret band region but shows an increased absorbance at 653 nm (see Table I). This latter observation is indicative of a cation-radical character for $[(TpivPP)Ni]^{3+}$. All the UV-visible data of (TpivPP)Ni and its reduction or oxidation products are summarized in Table I. In addition, the species produced after bulk electrolysis in CH_2Cl_2, 0.1 M TBAP at 1.35 V has an ESR signal centered at $g = 2.0025$ and a peak-to-peak width, ΔH_{pp}, of 6 G at 77 K. This ESR spectrum is shown in Figure 4 and clearly indicates a porphyrin π cation radical solution. Thus, both the spectroelectrochemical and ESR data are self-consistent and indicate that the product of the third electron abstraction from (TpivPP)Ni is the Ni(IV) cation radical $[(TpivPP)Ni^{IV}]^{3+}$ rather than the Ni(III) dication $[(TpivPP)Ni^{III}]^{3+}$.

Electroreduction of (TpivPP)Ni. Two possible products can be formed in the reduction of (TpivPP)Ni. These products differ in the site of electroreduction as shown by the two reaction pathways in Scheme III. The upper reduction pathway in Scheme III will produce a Ni(I) species, while the lower illustrated pathway will produce a Ni(II) anion radical. The electroreduction of nickel porphyrins generally leads to formation of Ni(II) porphyrin anion radicals,[10,15-18] but the formation of Ni(I) is also possible and has been demonstrated to occur after reduction of (OEiBC)Ni and (OEC)Ni, where OEiBC and OEC are the dianions of octaethylisobacteriochlorin and octaethylchlorin, respectively.[16-18] In the present study, the specific reduction pathway of (TpivPP)Ni and the products of electroreduction were determined by monitoring both the ESR and the UV-visible spectra during electro-

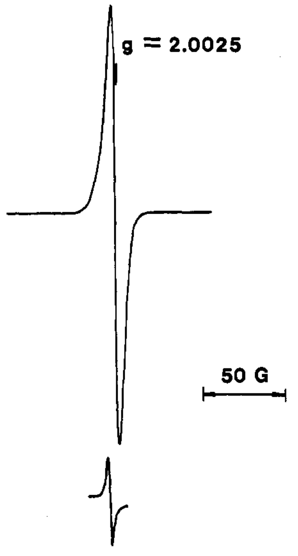

Figure 4. ESR spectrum obtained at −150 °C after bulk controlled-potential electrooxidation of (TpivPP)Ni at 1.35 V in CH_2Cl_2, 0.2 M TBAP.

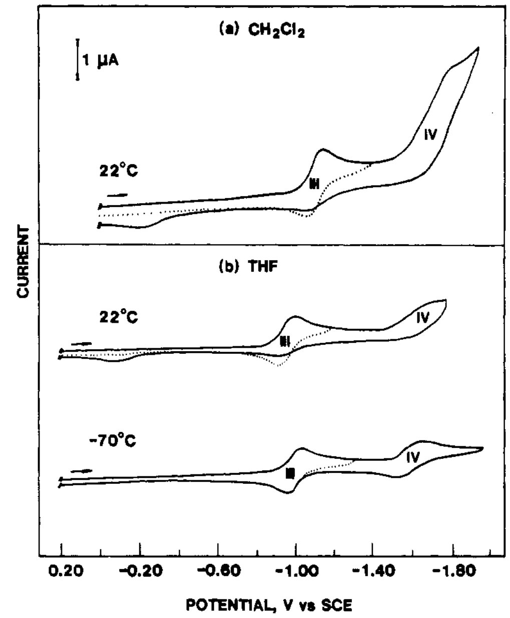

Figure 5. Cyclic voltammograms illustrating the reduction of 10^{-3} M (TpivPP)Ni: (a) in CH_2Cl_2, 0.1 M TBAP at 22 °C; (b) in THF, 0.1 M TBAP at 22 and −70 °C. Scan rate = 0.1 V/s.

---

(25) Erler, B. S.; Scholz, W. F.; Lee, Y. J.; Scheidt, W. R.; Reed, C. A. *J. Am. Chem. Soc.* **1987**, *109*, 2644..

(26) Lovecchio, F. V.; Gore, E. S.; Busch, D. H. *J. Am. Chem. Soc.* **1974**, *96*, 3109.

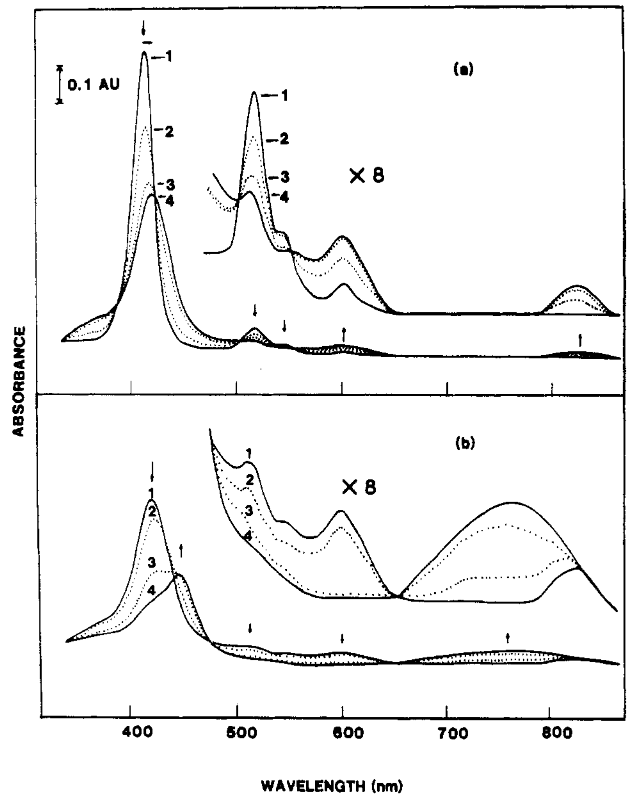

Figure 6. Potential-resolved spectral changes for solutions of (TpivPP)Ni in THF, 0.2 M TBAP: (a) during reduction at (1) 0.00, (2) −1.00, (3) −1.08, and (4) −1.20 V; (b) during further reduction at (1) −1.20 (2) −1.52, (3) −1.58, and (4) −1.63 V.

reduction of the complex in CH_2Cl_2 and THF.

Figure 5 shows cyclic voltammograms for electroreduction of (TpivPP)Ni in CH_2Cl_2 and THF containing 0.1 M TBAP. The compound undergoes two reductions in both solvents, and these are labeled as processes III and IV. The first reduction is reversible in both CH_2Cl_2 ($E_{1/2} = -1.12$ V) and THF ($E_{1/2} = -0.96$ V) when the cathodic scan is reversed at potentials positive of the second reduction. This is illustrated by the dotted line in Figure 5. The value of $|E_{pc} - E_{pa}|$ for process III is 70 ± 5 mV in both solvents, and $i_{pc}/v^{1/2}$ is constant at all scan rates between 0.05 and 0.50 V/s. In contrast, the second reduction of (TpivPP)Ni (process IV) is irreversible at room temperature in both CH_2Cl_2 and THF. In addition, a reoxidation peak appears after this reduction at $E_p = -0.22$ V in CH_2Cl_2 and at $E_p = -0.10$ V in THF (for a scan rate of 0.1 V/s). This oxidation peak is only present after scanning to potentials negative of peak IV and is most likely due to oxidation of an electrogenerated phlorin anion, which can be formed as an ultimate product in the overall reduction process IV at room temperature. The electrochemistry of phlorins has been discussed in the literature[27] and is not of interest in this present study. However, it can be noted that the second reduction of (TpivPP)Ni in THF is well defined by cyclic voltammetry at −70 °C (see Figure 5b). Under these conditions the separation between E_{pa} and E_{pc} is 110 mV at a scan rate of 0.1 V/s and a half-wave potential of $E_{1/2} = -1.59$ V is obtained.

Figure 6a shows the changes that occur in the electronic absorption spectra of (TpivPP)Ni in THF, 0.2 M TBAP as the potential is scanned between 0.00 and −1.20 V. The final spectrum is similar to other Ni(II) porphyrin anion radical spectra,[15,20] and the presence of seven isosbestic points indicates the absence of any spectrally detectable intermediate species. In contrast, the first reduction of (TpivPP)Ni in CH_2Cl_2, 0.2 M TBAP is not spectrally reversible and the electrochemically generated $[(TpivPP)Ni]^-$ reacts with CH_2Cl_2 on the time scale of thin-layer spectroelectrochemistry.

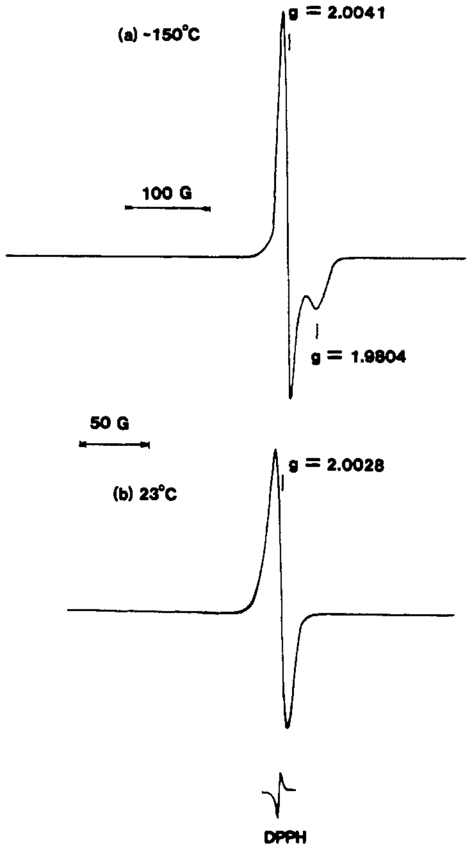

Figure 7. ESR spectra obtained after bulk controlled-potential electroreduction of (TpivPP)Ni at −1.2 V in THF, 0.2 M TBAP.

Dichloromethane has been shown to react with electrochemically generated $[(TPP)Co^I]$ porphyrins to form metal–carbon σ-bonded complexes as shown by the overall eq 1.[28] The reaction

$$[(TPP)Co^I]^- + CH_2Cl_2 \rightarrow (TPP)Co(CH_2Cl) + Cl^- \quad (1)$$

in eq 1 involves a two-electron oxidative addition and is similar to reactions observed between other Co(I) porphyrins and alkyl or aryl halides which lead to generation of the σ-bonded Co–carbon complex.[29,30] Similar types of reactions may also occur between CH_2Cl_2 and electroreduced (TpivPP)Ni. However, the initial porphyrin product of the reaction was not stable in this solvent and could not be characterized in solution.

Figure 7 shows the ESR spectra obtained after bulk controlled-potential electrolysis of (TpivPP)Ni in THF at −1.2 V. This potential corresponds to the first one-electron reduction of (TpivPP)Ni. At 23 °C, the ESR spectrum is isotropic while anisotropy contributes to the spectral behavior of $[(TpivPP)Ni]^-$ at −150 °C (see Figure 7). At 23 °C, $g = 2.0028$, but at −150 °C, $g_\perp = 2.0041$ and $g_\parallel = 1.9804$. The low-temperature spectrum in Figure 7 is similar to that of other reduced Ni tetrapyrrole complexes.[31] The spectrum has some Ni(I) character[31] but differs from the ESR spectrum of $[(OEiBC)Ni^I]^-$ in acetonitrile,[16,17] which is a genuine Ni(I) complex and has $g_\perp = 2.201$ and $g_\parallel = 2.073$.

UV-visible spectra taken during the second reduction of (TpivPP)Ni at −1.8 V in CH_2Cl_2, 0.1 M TBAP were not reproducible due in part to the reaction of $[(TpivPP)Ni]^-$ with CH_2Cl_2 and in part to the proximity of this reaction to the negative solvent limit (which is ∼−1.85 V). However, UV–vis spectra obtained during the second reduction in THF were reproducible. These potential resolved spectra are shown in Figure 6b. As seen in this

---

[27] (a) Lanese, J. G.; Wilson, G. S. *J. Electrochem. Soc.* **1972**, *119*, 1039. (b) Peychal-Heiling, G.; Wilson, G. S. *Anal. Chem.* **1971**, *43*, 550.

[28] Kadish, K. M.; Lin, X. Q.; Han, B. C. *Inorg. Chem.* **1987**, *26*, 4161.

[29] Guilard, R.; Lecomte, C.; Kadish, K. M. *Struct. Bonding* **1987**, *64*, 205–268.

[30] Guilard, R.; Kadish, K. M. *Chem. Rev.* **1988**, *88*, 1121–1146.

[31] Renner, M. W.; Forman, A.; Fajer, J.; Simpson, D.; Smith, K. M.; Barkigia, K. M. *Biophys. J.* **1988**, *53*, 277a.

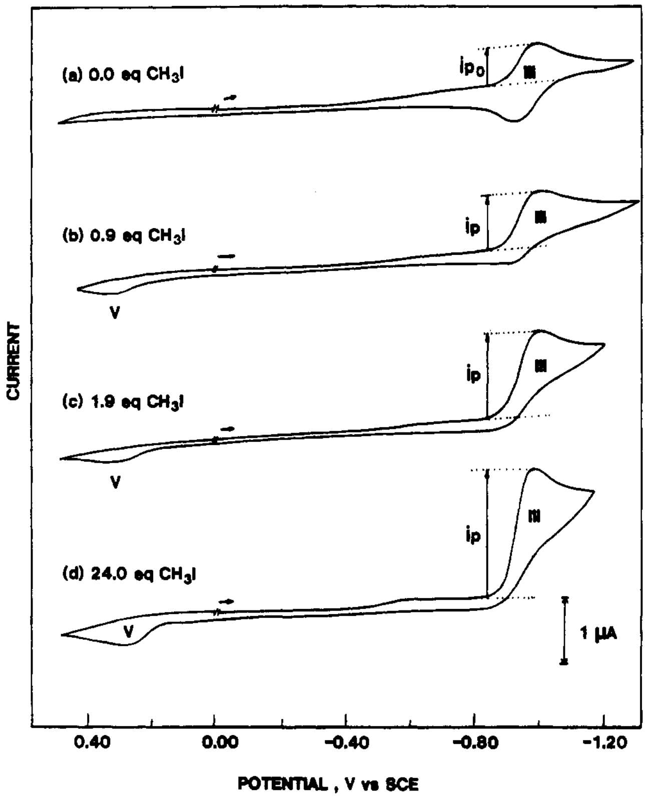

Figure 8. Cyclic voltammograms of (TpivPP)Ni in THF, 0.1 M TBAP at various CH_3I/porphyrin ratios (scan rate 0.10 V/s).

figure, the doubly reduced species has characteristics of both a porphyrin π dianion[15] and a phlorin.[27] The UV-visible data are given in Table I. The UV-visible and ESR spectra are thus self-consistent and indicate that the location of electron density is mostly on the porphyrin π ring system after the first electroreduction of (TpivPP)Ni. However, the fact that $[(TpivPP)Ni]^-$ catalytically reacts with CH_2Cl_2 at relatively low potentials could suggest that there is some Ni(I) character (electron density on the metal) in electroreduced (TpivPP)Ni, and a similar conclusion results from analysis of half-wave potentials for the two electroreductions. These reductions occur at $E_{1/2}$ values of -1.00 and -1.59 V in THF at -70 °C.

Reactivity of Electrogenerated $[(TpivPP)Ni]^-$ with CH_3I. Figure 8 shows cyclic voltammograms of (TpivPP)Ni in THF containing increasing concentrations of CH_3I. The first reduction is well defined in THF containing 0.1 M TBAP and occurs at $E_{1/2} = -0.96$ V. However, this reduction becomes progressively irreversible as the concentration of CH_3I in THF is increased. There is also a simultaneous enhancement in the magnitude of the cathodic peak current as well as the appearance of a new anodic peak, which occurs at $E_p = 0.30$ V on the reverse sweep for a scan of 0.1 V/s. This oxidation (peak V, Figure 8) is not present when the cathodic potential sweep is terminated before electrogeneration of $[(TpivPP)Ni]^-$. A peak at the same potential is observed after electrogeneration of $[(TPP)Co^I]^-$ in THF containing CH_3I and is due to oxidation of free I^- which is generated from CH_3I after reaction with the reduced form of the metalloporphyrin.[28]

The reductive electrochemistry of (TpivPP)Ni in the presence of CH_3I is similar to that of (TPP)Co,[28] (TPP)Fe,[32] and (OEiBC)Ni.[16,17] In all three cases, the singly reduced complex reacts with CH_3I and leads to the formation of I^- in solution. For the case of $[(TPP)Co^I]^-$ and $[(TPP)Fe^I]^-$ the ultimate porphyrin product is the σ-bonded (TPP)Co(R) or (TPP)Fe(R) species.[28-30] In contrast, a stable σ-bonded Ni(III) complex is not generated in the reaction between $[(TpivPP)Ni]^-$ and CH_3I. The initial product of this reaction is unstable and leads to a re-formation of the intial Ni(II) species, which is then rereduced to give $[(TpivPP)Ni]^-$. Thus, the overall reaction involves a catalytic reduction of CH_3I. A similar catalytic reduction of CH_3I occurs upon reaction with $[(OEiBC)Ni^I]^-$ and, in this case, was postulated to generate a transient σ-bonded $(OEiBC)Ni(CH_3)$ complex before re-formation of the initial (OEiBC)Ni derivative, CH_4, and other unidentified non-porphyrin products.[17]

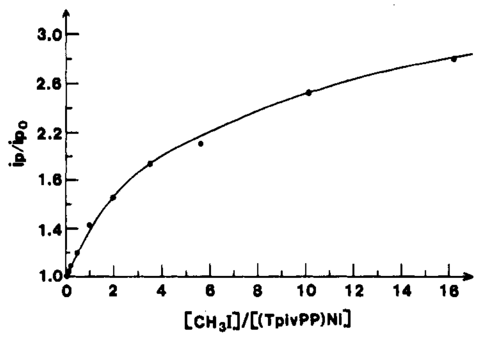

Figure 9. Plot of i_p/i_{p_0} as a function of $[CH_3I]/[(TpivPP)Ni]$ in THF, 0.1 M TBAP. Values of i_p and i_{p_0} are given in Figure 8.

Bulk electrolysis of (TpivPP)Ni proceeds smoothly at -1.2 V in THF containing 0.2 M TBAP and gives n values of 1.05 ± 0.01 electrons. However, the limiting current decreases more slowly upon the addition of 10-30 equiv of CH_3I and does not approach a limit of zero. The ^1H NMR spectrum of the isolated compound[33] after the reaction with CH_3I exhibits ^1H NMR features of (TpivPP)Ni and thus also indicates a regeneration of the initial Ni(II) complex.

A plot of i_p/i_{p_0} vs $[CH_3I]/[(TpivPP)Ni]$ is shown in Figure 9, where i_p and i_{p_0} are the measured peak currents for process III in the presence and absence of CH_3I. The peak current for reduction of (TpivPP)Ni increases with increasing concentrations of CH_3I. This behavior and the lack of a coupled anodic peak for process III are consistent with an electrocatalytic reduction and are similar to trends observed during the catalytic reduction of n-butyl bromide by iron porphyrins.[34]

A chemical reaction also occurs between CH_3I and other reduced Ni(II) porphyrins such as $[T(p\text{-}Et_2N)PP]Ni$ and (TRP)Ni where R = Me, Et, or Pr. Thus, the reactivity of electrogenerated $[(TpivPP)Ni]^-$ is not unusual for a reduced Ni porphyrin and is similar to the suggested function of activated F_{430}—a Ni(I) hydrocorphinoid in methyl coenzyme M reductase.[35,36]

The electrochemistry of (TpivPP)Ni is also unusual with respect to its oxidative properties, and the compound provides the first example of an electrogenerated Ni(IV) cation radical. The ability to access this high oxidation state is clearly related to the presence of the "picket fence". A similar accessing of high oxidation states might also be possible for other transition-metal "picket fence" complexes containing Mn, Cr, or Co central metals. Studies of these compounds are presently under investigation.

Acknowledgment. The support of the National Science Foundation (Grants CHE-8515411 and INT-8413696) is gratefully acknowledged. K.M.K. and R.G. also acknowledge NATO for partial support of this work.

Registry No. (TpivPP)Ni, 120120-01-6; $[(TpivPP)Ni]^{2+}$, 120120-02-7; $[(TpivPP)Ni]^{3+}$, 120120-03-8; $[(TpivPP)Ni]^-$, 120120-04-9; CH_3I, 74-88-4; TBAP, 1923-70-2; $(TBA)PF_6$, 3109-63-5.

---

(32) Lexa, D.; Mispelter, J.; Savéant, J.-M. *J. Am. Chem. Soc.* **1981**, *103*, 6806.

(33) The compound workup was as follows: 5×10^{-4} M (TpivPP)Ni was reduced by controlled-potential electrolysis in 0.2 M TBAP, after which 10^{-1} M CH_3I was added to the solution. The mixture was stirred in the dark for 1-2 h in the absence of oxygen and then evaporated to dryness, after which 1 mL of C_6D_6 was added to the flask before obtaining the NMR spectrum.

(34) Lexa, D.; Savéant, J.-M.; Wang, D. L. *Organometallics* **1986**, *5*, 1428.

(35) Jaun, B.; Pfaltz, A. *J. Chem. Soc., Chem. Commun.* **1988**, 293.

(36) Nagle, D. P.; Wolfe, R. S. *Proc. Natl. Acad. Sci. U.S.A.* **1983**, *80*, 2151.